Neuron, Vol. 19, 665–678, September, 1997, Copyright ©1997 by Cell Press

Tonic Synaptic Inhibition Modulates Neuronal Output Pattern and Spatiotemporal Synaptic Integration

Michael Häusser* and Beverley A. Clark
Laboratoire de Neurobiologie
Ecole Normale Supérieure
46 Rue d'Ulm
75005 Paris
France

Summary

Irregular firing patterns are observed in most central neurons in vivo, but their origin is controversial. Here, we show that two types of inhibitory neurons in the cerebellar cortex fire spontaneously and regularly in the absence of synaptic input but generate an irregular firing pattern in the presence of tonic synaptic inhibition. Paired recordings between synaptically connected neurons revealed that single action potentials in inhibitory interneurons cause highly variable delays in action potential firing in their postsynaptic cells. Activity in single and multiple inhibitory interneurons also significantly reduces postsynaptic membrane time constant and input resistance. These findings suggest that the time window for synaptic integration is a dynamic variable modulated by the level of tonic inhibition, and that rate coding and temporal coding strategies may be used in parallel in the same cell type.

Introduction

Most neurons in the intact brain display an irregular firing pattern both at rest and during the response to external stimuli. An understanding of the way in which this irregular firing pattern is generated is likely to lead to significant insights into how neurons process information (reviewed by Shadlen and Newsome, 1994; Softky, 1995; Rieke et al., 1997). In particular, it is hoped that by studying the mechanisms that underlie the irregular pattern of activity, we can gain an understanding of the way in which neurons transform synaptic input into output. Recent modeling studies have focused on two competing explanations. One view (Abeles, 1991; Softky and Koch, 1993; Softky, 1994; König et al., 1996) holds that the irregular firing pattern reflects "coincidence detection" of synchronous excitatory inputs, possibly amplified by active dendritic properties. According to this hypothesis, the temporal structure of the output pattern reflects precisely the pattern of synaptic inputs. On the other hand, it has been shown that highly irregular firing patterns can be produced by a continuous barrage of uncorrelated excitatory and inhibitory inputs that are "balanced," such that the neuron fires spikes at random due to its proximity to threshold (Shadlen and Newsome, 1994; Bell et al., 1995; Troyer and Miller, 1997; Jaeger et al., 1997). This has been interpreted to mean that information is transmitted by the average action potential frequency (a "rate code"), the precise timing of action potentials being irrelevant (Shadlen and Newsome, 1994). Central to this debate is the timescale over which synaptic inputs are integrated. An important determinant of this timescale is the membrane time constant, which governs the decay of propagated synaptic potentials and thus also their summation. Unfortunately, the value of the membrane time constant in vivo remains unknown, and current theoretical predictions are limited by major uncertainties about the electrical properties of neurons and the rate and efficacy of individual synaptic inputs.

We have addressed these issues by examining the properties and interactions of two classes of GABAergic neurons in the cerebellar cortex: Purkinje cells, which form the sole output of the cerebellar cortex, and interneurons in the molecular layer. Neurons of both types fire action potentials in an irregular pattern during the execution of movements and when the animal is at rest (Granit and Phillips, 1956; Eccles et al., 1967; Armstrong and Rawson, 1979). The way in which intrinsic membrane properties and the pattern of synaptic inputs interact to generate the output of these neurons is unknown. Since the dendrites and axons of these neurons are arranged in a highly planar manner (Palay and Chan-Palay, 1974), much of the circuitry of the molecular layer can be preserved in a slice preparation, where synaptic transmission can be manipulated with ease. By making recordings in cerebellar slices, we have found that even in the absence of excitatory synaptic transmission, both interneurons and Purkinje cells are spontaneously active. We demonstrate that single action potentials in an inhibitory interneuron can generate variable delays in action potential firing in its postsynaptic cells, and that the overall activity of the interneuron network produces an irregular firing pattern in both neuronal types. Furthermore, we show that the tonic postsynaptic conductance generated by spontaneous interneuron activity has an important influence on synaptic integration.

Results

Spontaneous Activity in Purkinje Cells and Interneurons

We used two noninvasive recording techniques, extracellular recording and cell-attached patch-clamp recording, to measure the activity of single Purkinje cells and molecular layer interneurons in cerebellar slices at temperatures close to those occurring in vivo. For both cell types, virtually all cells recorded (>98%) fired action potentials spontaneously under control conditions (Figures 1A and 1D). The firing rates of active neurons ranged from 1–148 Hz for Purkinje cells (Figure 1C) and 1–41 Hz for interneurons (Figure 1F). The mean firing rates were 38.8 ± 2.4 Hz for Purkinje cells (n = 106; 16 extracellular recordings and 90 cell-attached recordings) and 12.3 ± 0.9 Hz for interneurons (n = 76; 9 extracellular

*Address correspondence to: Dr. M. Häusser, Department of Physiology, University College London, Gower Street, London WC1E 6BT, United Kingdom.

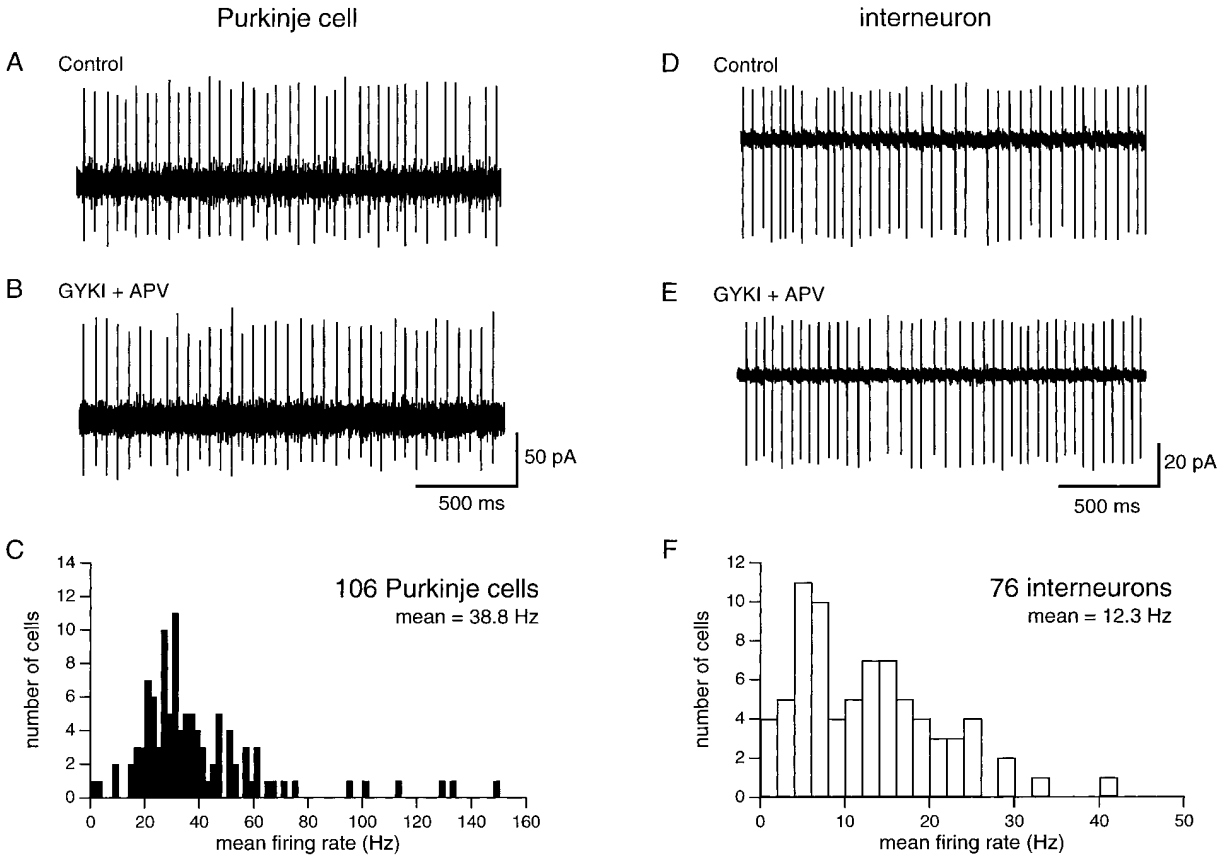

Figure 1. Spontaneous Activity in Purkinje Cells and Interneurons

(A and B) Extracellular recording from a cerebellar Purkinje cell. The mean firing rate was 19.0 Hz under control conditions (A). Addition of GYKI 52466 (100 μM) and D-APV (50 μM) reduced the mean firing rate to 18.3 Hz (B).

(C) Histogram of mean firing rates in 106 Purkinje cells recorded with cell-attached or extracellular pipettes under control conditions.

(D and E) Cell-attached recording from a molecular layer interneuron (75 μm from the Purkinje cell layer); the mean firing rate was 20.2 Hz under control conditions (D). Addition of GYKI 52466 (100 μM) and D-APV (50 μM) reduced the mean firing rate to 19.7 Hz (E).

(F) Histogram of the mean firing rates of 76 interneurons recorded with cell-attached or extracellular pipettes under control conditions.

recordings and 67 cell-attached recordings). No significant difference was found between the firing rate of interneurons located in the inner molecular layer (somata ≤60 μm from the Purkinje cell layer), compared to more distal interneurons (somata >60 μm from the Purkinje cell layer; $p > 0.7$), suggesting that interneurons with basket and stellate-type axons (Palay and Chan-Palay, 1974) have similar firing rates under these experimental conditions.

To determine whether transmitter release from glutamatergic terminals could contribute to the resting firing rate of Purkinje cells and interneurons, we applied two excitatory amino acid antagonists: GYKI 52466 (50–100 μM) to block AMPA-type glutamate receptors (Donevan and Rogawski, 1993; Zorumski et al., 1993; we avoided quinoxalinedione antagonists since they can excite interneurons: McBain et al., 1992) and D-APV (50 μM) to block N-methyl-D-aspartic acid receptors. Concurrent application of both antagonists only reduced the resting firing rate of Purkinje cells and interneurons by 11 ± 9% ($n = 6$; $p > 0.7$) and 1 ± 7% ($n = 7$; $p > 0.8$) of the control value, respectively (see Figures 1B and 1E). To evaluate the contribution of tonic activation of metabotropic glutamate receptors (mGluR) to the spontaneous firing, we applied the nonselective mGluR antagonist (+)-α-methyl-4-carboxyphenylglycine (0.5–1 mM; Bashir et al., 1993). In the presence of the antagonist, there was no significant change in the firing rate of Purkinje cells (2 ± 4% decrease relative to control; $n = 4$; $p > 0.8$) and interneurons (1 ± 11% decrease relative to control; $n = 4$; $p > 0.8$). These findings demonstrate that both Purkinje cells and interneurons fire action potentials spontaneously in the absence of glutamatergic synaptic excitation.

Effect of Tonic Inhibition on the Rate and Pattern of Purkinje Cell and Interneuron Output

To investigate the effect of spontaneous firing of inhibitory neurons on the firing pattern of other neurons in the network, cell-attached and extracellular recordings were made from Purkinje cells and interneurons, and synaptic inhibition was blocked using the $GABA_A$ receptor antagonists SR 95531 (gabazine, 10–30 μM; Hamann et al., 1988; Ueno et al., 1997), bicuculline (30 μM), or picrotoxin (30 μM). Results using these antagonists were indistinguishable, and therefore the data were pooled. When inhibition was blocked, the mean firing rate of

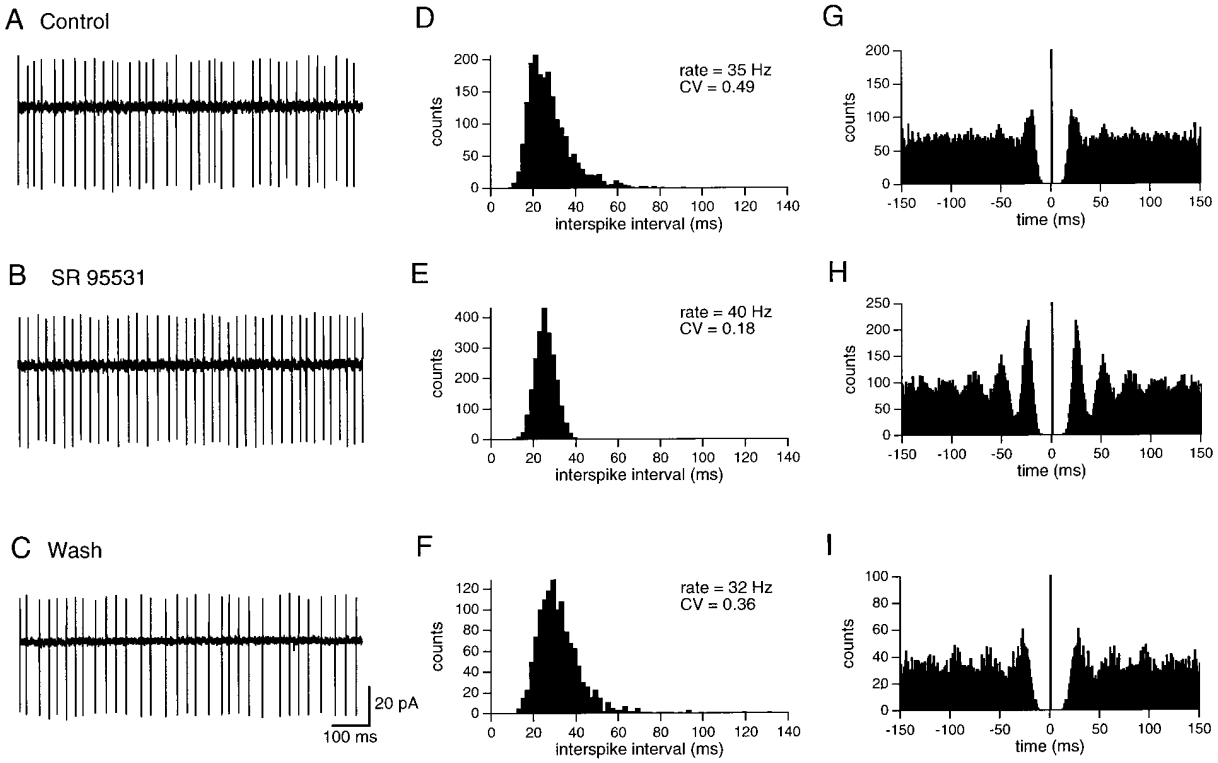

Figure 2. Blocking Tonic Inhibition Transforms the Irregular Firing Pattern of Purkinje Cells into a Regular Pattern

(A–C) Cell-attached patch-clamp recording from a Purkinje cell in before (A), during application of 10 μM SR 95531 (B), and after washout (C). In the presence of SR 95531 (B), the firing rate increases, and the action potentials become much more regular.

(D–F) Interspike interval histograms from the corresponding recordings in (A) through (C). The mean firing rate and the CV under the different conditions are given. Note the narrow, symmetric distribution of the interspike intervals during application of SR 95531 (E).

(G–I) Autocorrelation of action potential trains from the corresponding recordings in (A) through (C). Note that multiple distinct peaks are visible in the autocorrelogram when inhibition is blocked (I).

both Purkinje cells and interneurons increased by 41 ± 9% ($n = 25$; $p < 0.01$) and 55 ± 21% ($n = 15$; $p < 0.01$), respectively, relative to control, indicating that both of these cell types are subject to tonic synaptic inhibition.

The firing patterns of Purkinje cells and interneurons were highly irregular under control conditions. The interspike interval (ISI) distribution showed a long tail for both cell types (Figures 2 and 3), and the coefficient of variation (CV) of the ISI was substantial, being 0.28 ± 0.038 in Purkinje cells (range: 0.05–1.13; $n = 68$) and 0.51 ± 0.024 in interneurons (range: 0.19–0.85; $n = 43$). Bursting patterns of activity were not observed in interneurons, and only rarely in Purkinje cells (<5% of cells). When inhibition was blocked, the firing pattern of both Purkinje cells and interneurons became strikingly regular. This was reflected in the ISI histogram, which became a single narrow peak with a Gaussian shape (Figures 2E and 3E). The CV of the ISI was significantly reduced in both Purkinje cells and interneurons, being 0.10 ± 0.009 ($n = 25$; $p < 0.01$) and 0.24 ± 0.04 ($n = 15$; $p < 0.01$), respectively, when inhibition was blocked. Another index of the regularity of firing, the autocorrelogram, which typically showed only one or two peaks in control conditions (Figures 2G and 3G), developed multiple clearly defined peaks when inhibition was blocked (Figures 2H and 3H). All of these effects were reversible upon washout of the antagonist.

Spontaneous Synaptic Currents in Purkinje Cells and Interneurons

To determine the nature of the spontaneous synaptic input to Purkinje cells and interneurons, synaptic currents were recorded using the whole-cell patch-clamp method. Purkinje cells were maintained at −70 to −80 mV, and a chloride-rich internal solution was used to maximize driving force through $GABA_A$ receptor channels (Figure 4A). The rate of spontaneous synaptic currents measured under these conditions was 143.5 ± 36.4 Hz ($n = 6$). To estimate the contribution of excitatory synaptic currents to the spontaneous activity, inhibitory events were blocked with the $GABA_A$ receptor antagonists SR 95531 (50 μM) and picrotoxin (50 μM). The remaining synaptic currents (Figure 4B), which occurred at a rate of 11.4 ± 4.5 Hz ($n = 4$), were completely blocked by addition of GYKI 52466 and D-APV (Figure 4C), indicating that they are mediated by ionotropic glutamate receptor channels.

Owing to the very favorable signal-to-noise ratio in recordings from interneurons (Llano and Gerschenfeld, 1993), we distinguished excitatory and inhibitory synaptic activity under control conditions by using a low-chloride potassium gluconate internal solution to separate the reversal potentials of excitatory and inhibitory synaptic currents. Under these conditions, when interneurons were voltage-clamped at −35 to −40 mV,

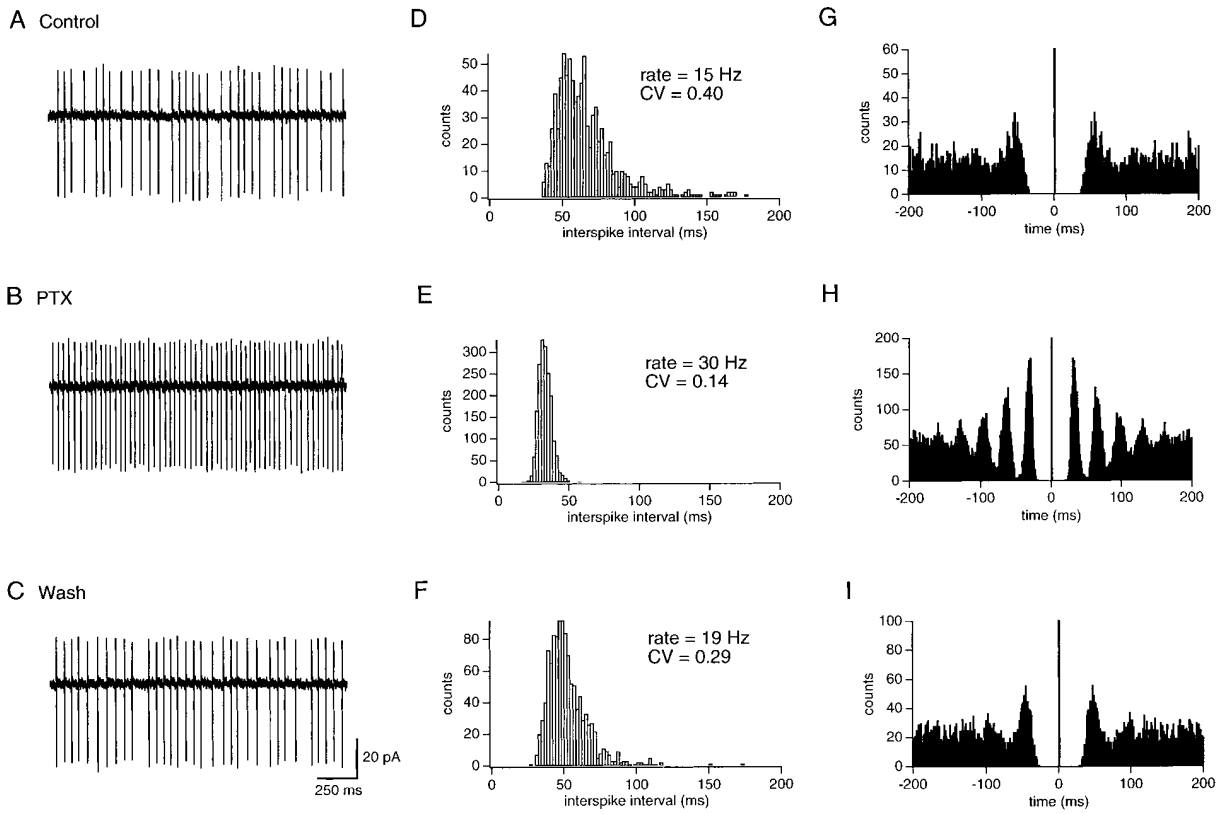

Figure 3. Blocking Tonic Inhibition Transforms the Irregular Firing Pattern of Interneurons into a Regular Pattern

(A–C) Cell-attached patch-clamp recording from a molecular layer interneuron (100 μm from the Purkinje cell layer) under control conditions (A), during application of 30 μM picrotoxin (B), and after washout of the drug (C).

(D–F) Interspike interval histograms from the recordings in (A) through (C), with the mean firing rates and the CV indicated.

(G–I) Autocorrelation of action potential trains from the corresponding recordings in (A) through (C). Blockade of inhibition caused a marked increase in the regularity of firing, as shown by the multiple peaks in the autocorrelogram (H).

excitatory events appeared as inward currents, and inhibitory events appeared as outward currents (Figure 4D). The outward currents were sensitive to SR 95531 (30–50 μM; Figure 4F) or picrotoxin (50 μM), indicating that they were due to activation of $GABA_A$ receptors. The frequency of spontaneous inhibitory currents in interneurons was 18.1 ± 3.2 Hz (n = 8), and the frequency of excitatory currents was 1.6 ± 0.9 Hz (n = 8). To separate the contribution of action potential-dependent and -independent (quantal) transmitter release, the frequency of spontaneous currents was measured in tetrodotoxin, and averaged 3.9 ± 1.5 Hz (n = 8) for inhibitory currents and 1.3 ± 0.5 Hz (n = 8) for excitatory currents.

These findings indicate that spontaneous synaptic input to both cell types is predominantly inhibitory and mediated by $GABA_A$ receptors. Furthermore, ~80% of the spontaneous inhibitory currents result from action potential–dependent release of GABA. An estimate of the synaptic convergence of inhibitory neurons can be obtained by dividing the action potential–dependent IPSC rate by the mean firing rate of the interneurons. This gives a convergence of at least nine interneurons presynaptic to every Purkinje cell and at least one to two interneurons presynaptic to every interneuron. These estimates represent lower limits due to failures in transmission, detection failures, and axon truncation by the slicing procedure; the Purkinje cell estimate is comparable to the ~10:1 ratio of the number of interneurons to Purkinje cells in the molecular layer of rat cerebellar cortex (Korbo et al., 1993).

Inhibition of Action Potential Firing in Purkinje Cells and Interneurons by Single Presynaptic Interneurons

To assess the contribution of single presynaptic interneurons to the generation of the irregular firing patterns, simultaneous whole-cell patch-clamp recordings were made from interneurons and synaptically connected Purkinje cells or interneurons. Interneuron action potentials were timed to occur reproducibly following an action potential in the connected postsynaptic cell (see Figure 5). A single presynaptic interneuron action potential could significantly delay subsequent action potentials in the postsynaptic cell. In Purkinje cells, the mean interspike interval following a presynaptic interneuron action potential was increased by 12.1 ± 3.8% on average (n = 7; range: 2%–24%) relative to the control value (Figures 5A and 5B). A similar effect was found with postsynaptic interneurons (Figures 5E and 5F), where the mean ISI was increased by 15.6 ± 2.7% on average (n = 8; range: 7%–29%). The mean amplitude of the IPSP made by single interneurons was variable

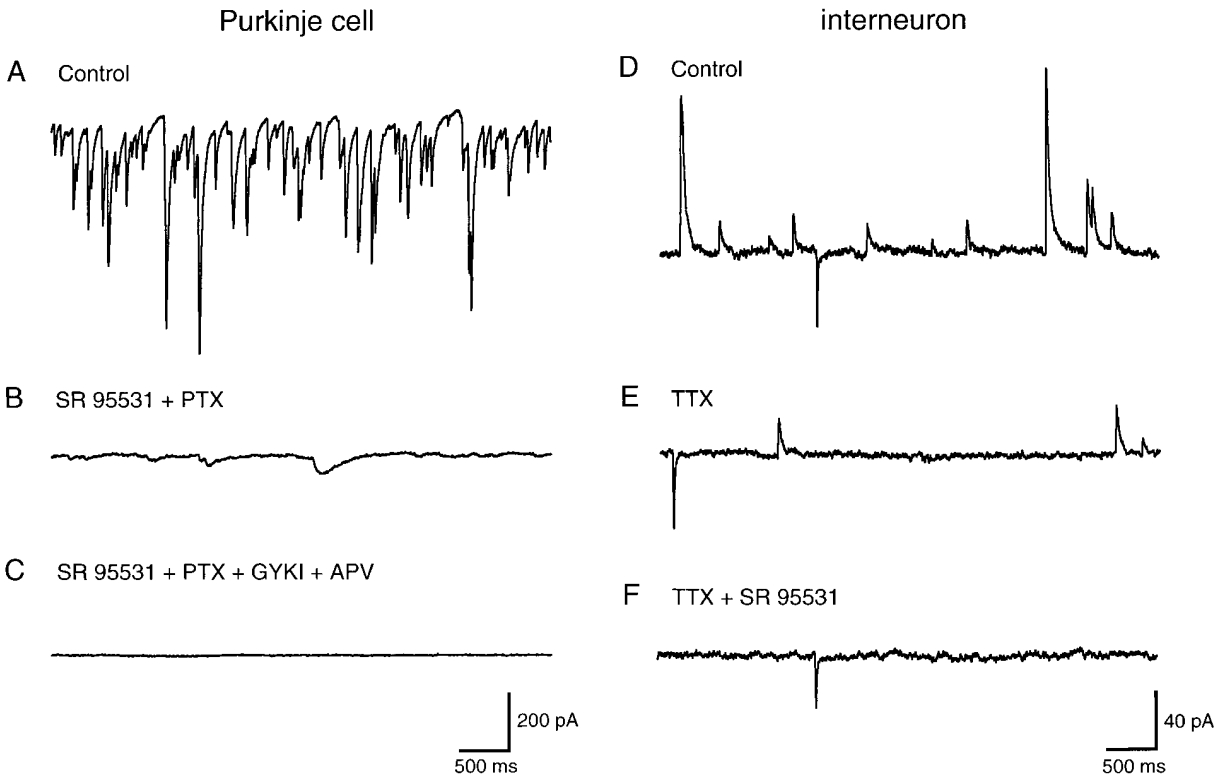

Figure 4. Spontaneous Synaptic Activity in Purkinje Cells and Interneurons

(A–C) Whole-cell recording from a Purkinje cell using a high Cl^- internal solution at a holding potential of −70 mV. In control conditions (A), a high rate of spontaneous activity was seen (210 Hz), which was reduced to 13 Hz in the presence of 50 μM SR 95531 and 50 μM picrotoxin (PTX) (B). All detectable synaptic activity was blocked when 100 μM GYKI 52466 and 50 μM D-APV were added to the solution containing the $GABA_A$ antagonists (C).

(D–F) Whole-cell recording from a molecular layer interneuron (85 μm from the Purkinje cell layer) using a K-gluconate internal solution. In control conditions at a holding potential of −40 mV, inhibitory synaptic currents (upward deflections) occurred at a rate of 15.7 Hz, and excitatory synaptic currents (downward deflections) occurred at a rate of 0.4 Hz. Addition of tetrodotoxin (TTX, 1 μM) reduced the rate of inhibitory and excitatory events to 2.0 Hz and 0.3 Hz, respectively. Finally, all outward synaptic currents were blocked following the further addition of 30 μM SR 95531 (F), confirming their identity as inhibitory synaptic currents mediated by $GABA_A$ receptors.

from connection to connection, and ranged from 0.05–0.61 mV (mean: 0.24 ± 0.08 mV) in Purkinje cells and 0.30–1.65 mV (mean: 0.90 mV ± 0.17 mV) in interneurons at a holding potential of ∼−60 mV. The mean increase in the postsynaptic ISI generated by a single interneuron spike was highly correlated with the mean IPSP amplitude ($r = 0.91$ for postsynaptic Purkinje cells and 0.83 for postsynaptic interneurons).

The delay in postsynaptic action potential firing caused by an interneuron action potential was highly variable from trial to trial in the same cell: in some trials, the interspike interval was indistinguishable from that in control, and in others, the action potential could be delayed as much as 15–20 ms (see Figures 5B and 5F). This was quantified by calculating the CV of the interspike interval. In the absence of the presynaptic spike, the CV in the timing of action potentials averaged 0.084 ± 0.008 in Purkinje cells and 0.11 ± 0.011 in interneurons. The CV increased to 0.115 ± 0.019 in Purkinje cells and 0.148 ± 0.010 in interneurons following an action potential in a presynaptic interneuron. The IPSP resulting from an action potential in a presynaptic interneuron also fluctuated substantially from trial to trial (Figures 5C and 5G; see also Vincent and Marty, 1996). At a given connection, the postsynaptic interspike interval was well correlated with the amplitude of the IPSP triggered within that particular interval (Figures 5D and 5H), suggesting that the increased variability in the ISI following the interneuron spike is directly related to the trial-to-trial variability in the IPSP amplitude.

Tonic Synaptic Inhibition Modulates Cable Properties

We have shown that tonic synaptic inhibition causes substantial changes in the spontaneous firing patterns of Purkinje cells and interneurons. Since these neurons also generate action potentials in response to activation of excitatory synapses, it is important to determine the effect of tonic inhibition on the integration of synaptic input. This is to a large extent determined by the passive cable properties of the neuron (Rall, 1967; Jack et al., 1983; Spruston et al., 1994). To measure the effect of the conductance generated by interneuron activity on the cable properties of Purkinje cells and interneurons, we compared the input resistance and membrane time constant of these neurons in the presence and absence of tonic inhibition. Apparent membrane time constant

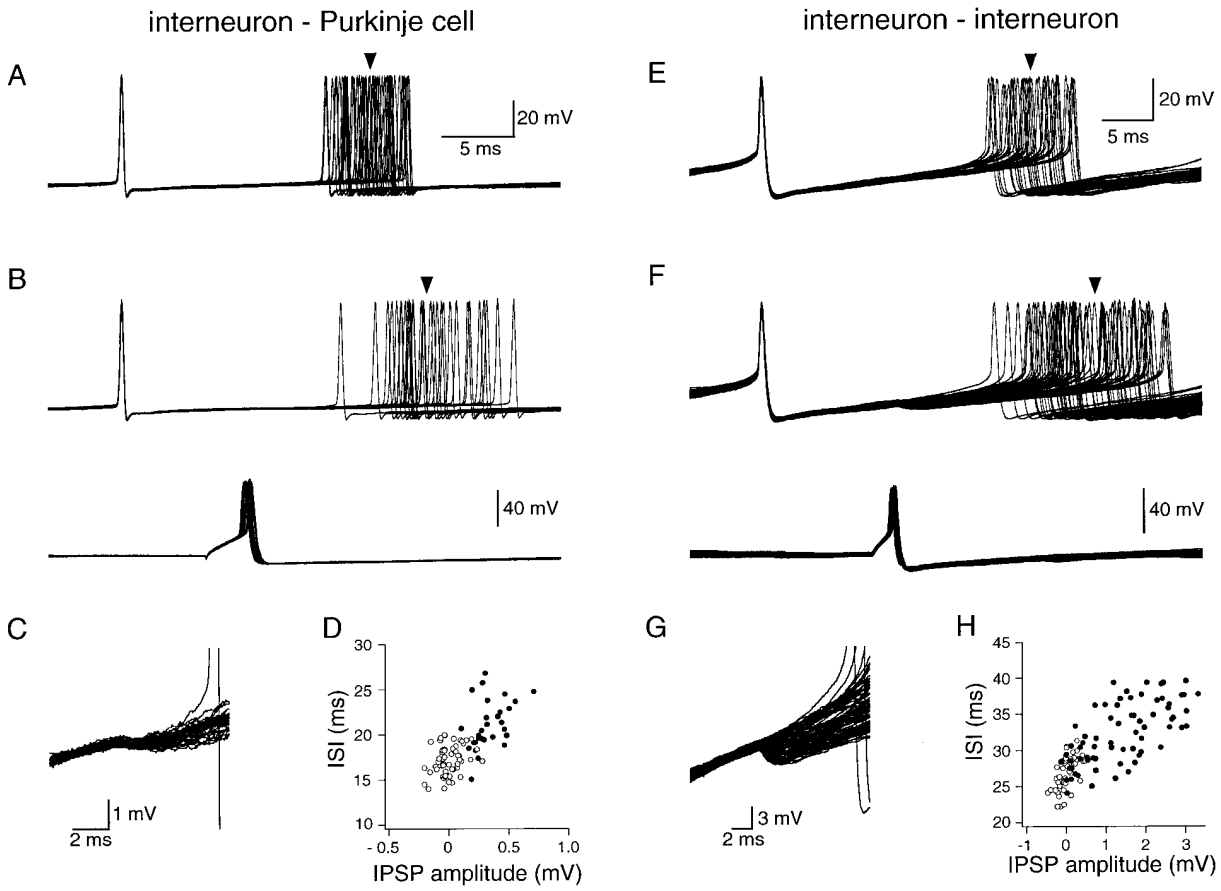

Figure 5. Single Interneurons Cause Variable Delays in Postsynaptic Spike Timing

(A–D) Simultaneous recording from an interneuron and a synaptically connected Purkinje cell. In (A), pairs of spontaneous action potentials in the Purkinje cell are aligned on the peak of the first action potential. The mean ISI was 17.2 ± 0.2 ms (n = 60 intervals), and is indicated by an arrowhead. In (B), a single spike in the presynaptic interneuron (lower traces) was triggered to occur in between the two Purkinje cell action potentials (upper traces). The resulting IPSP delayed the succeeding Purkinje cell action potential, with the mean ISI being 21.1 ± 0.5 ms (n = 30; $p < 0.01$). Sweeps where spontaneous synaptic potentials were detected were excluded from (A) and (B). An expanded view of the IPSPs in the Purkinje cell caused by the presynaptic action potential is shown in (C). In (D), the relationship between the IPSP amplitude (absolute value) and the resulting ISI is shown. IPSP amplitudes (closed circles) were measured as the difference in voltage at the time point of the presynaptic spike to the voltage at the time point of the peak of the averaged IPSP. The same measurement was done on sweeps lacking a presynaptic action potential (open circles); all amplitudes were normalized to the mean of the control amplitudes. The correlation coefficient for the IPSP amplitudes versus the ISIs (D) was 0.41.

(E–H) Same experiment as in (A) through (D) at an interneuron–interneuron connection. The mean ISI was 26.7 ± 0.3 ms (n = 47) in control (E), and 32.9 ± 0.6 ms (n = 77; $p < 0.01$) with the interneuron spike (F). The postsynaptic IPSPs in (F) are shown at higher magnification in (G). The correlation coefficient for the IPSP amplitudes versus the ISIs (H) was 0.65.

(τ_0) and input resistance (R_{in}) were measured at subthreshold potentials using brief (0.5 ms) current pulses, thus minimizing the contribution of voltage-gated conductances. The mean value of τ_0 was 35.4 ± 2.9 ms in Purkinje cells (n = 25) and 9.4 ± 1.5 ms in interneurons (n = 15). As shown in Figures 6A and 6B, when inhibition mediated by $GABA_A$ receptors was blocked, τ_0 increased substantially, to 79.5 ± 6.2 ms in Purkinje cells (n = 15; $p < 0.01$) and 13.1 ± 2.7 ms in interneurons (n = 9; $p < 0.01$). Similar changes were also observed in the apparent R_{in} when inhibition was blocked. Under control conditions, R_{in} was 49.5 ± 6.8 MΩ in Purkinje cells and 643 ± 96 MΩ in interneurons, and increased to 121 ± 17.4 MΩ ($p < 0.01$) and 871 ± 97 MΩ ($p < 0.01$), respectively, in the presence of $GABA_A$ antagonists. Addition of GYKI 52466 (100 μM) and D-APV (50 μM) to block ionotropic glutamate receptors had little further effect on either τ_0 or R_{in} in the presence of $GABA_A$ antagonists (τ_0 increased by 13 ± 6% and 15 ± 17%, and R_{in} increased by 13 ± 10% and 7 ± 2% in 9 Purkinje cells and 8 interneurons, respectively). These findings indicate that spontaneous activity in the interneuron population generates a postsynaptic conductance, which significantly affects cable properties.

Activity in Single Interneurons Can Modulate Cable Properties

To determine the ability of single interneurons to change postsynaptic τ_0 and R_{in}, simultaneous patch-clamp recordings were made from synaptically connected interneuron–Purkinje cell and interneuron–interneuron pairs.

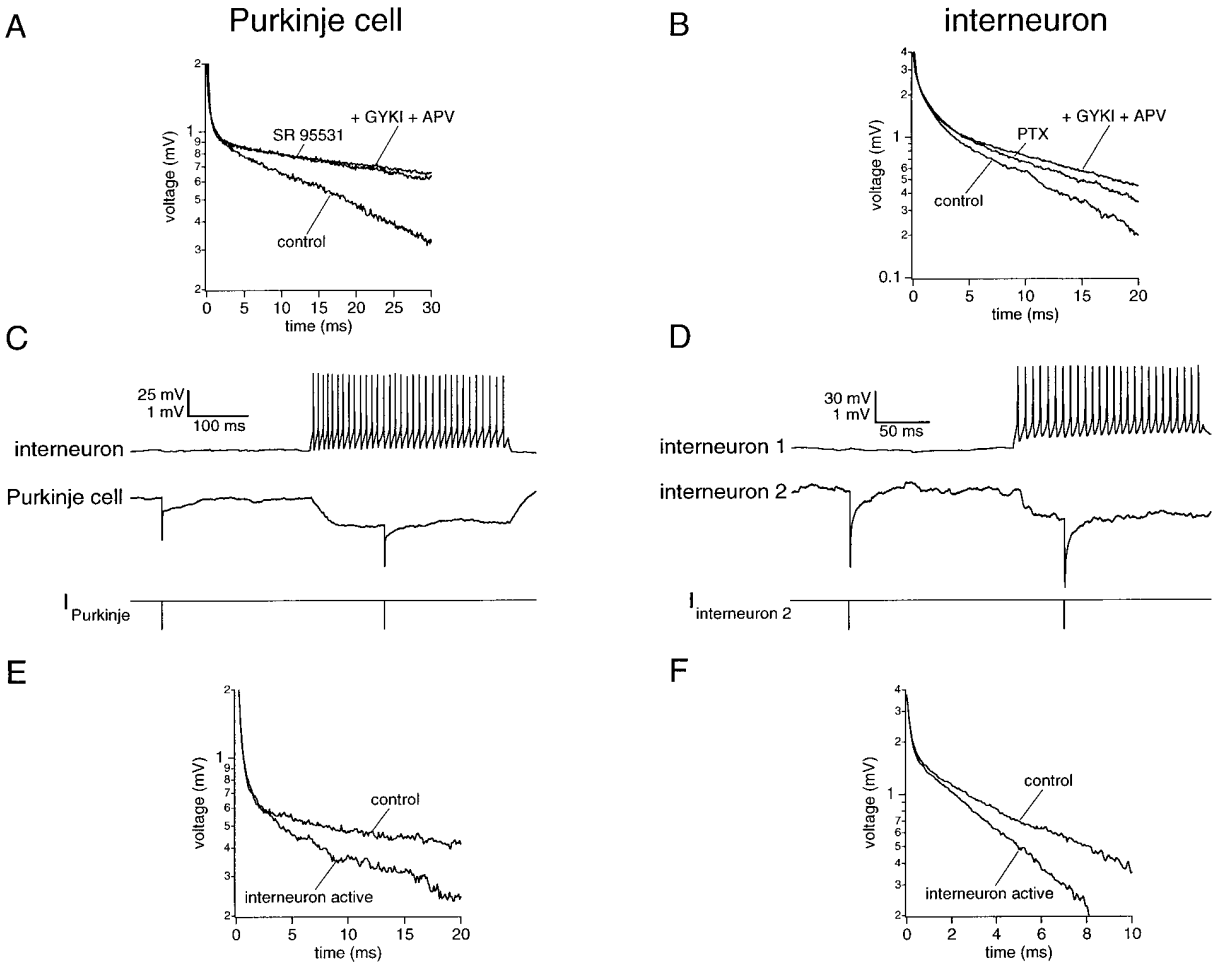

Figure 6. Effect of Activity in Single and Multiple Interneurons on Postsynaptic Cable Properties

(A and B) Effect of activity in the interneuron network on the cable properties of a Purkinje cell (A) and an interneuron (B) located 70 μm from the Purkinje cell layer. (A) and (B) show semilogarithmic plots of the averaged and normalized voltage transients in response to brief (0.5 ms) positive and negative pulses. In control conditions, the apparent τ_0 of the Purkinje cell was 29 ms, and the apparent R_{in} was 60 MΩ. In the presence of SR 95531 (10 μM), τ_0 and R_{in} were increased to 77 ms and 141 MΩ, respectively, and after further addition of GYKI 52466 (100 μM) and D-APV (50 μM) increased to 86 ms and 162 MΩ, respectively. For the interneuron responses shown in (B), τ_0 was 16 ms, and R_{in} was 815 MΩ in control conditions. These values increased to 23 ms and 938 MΩ, respectively, in the presence of picrotoxin (30 μM), and to 24 ms and 970 MΩ, respectively, after addition of GYKI 52466 (100 μM) and D-APV (50 μM).

(C and D) Simultaneous recording from a presynaptic interneuron and a synaptically connected Purkinje cell (C) or interneuron (D). The presynaptic interneurons (located 45 μm and 100 μm from the Purkinje cell layer, respectively) were held at −60 to −65 mV and depolarized to generate a train of action potentials. The top traces show a single representative sweep of the activity in the presynaptic interneurons. The middle traces show averaged responses in the Purkinje cell (C) and the postsynaptic interneuron (D) to two identical brief current pulses (0.5 ms; −1.0 nA in the Purkinje cell, −0.05 nA in the postsynaptic interneuron) injected into the postsynaptic cells while the presynaptic interneuron was silent and while it was active; the postsynaptic current injections are illustrated schematically below the postsynaptic traces.

(E and F) Semilogarithmic plots of the averaged and normalized voltage responses to positive and negative current pulses from the experiments shown in (C) and (D), respectively. For the postsynaptic Purkinje cell (E), τ_0 was 53 ms, and R_{in} was 66 MΩ under control conditions, decreasing to 25 ms and 29 MΩ during activity in the presynaptic interneuron. For the postsynaptic interneuron (F), located 140 μm from the Purkinje cell layer, τ_0 was 9.1 ms, and R_{in} was 475 MΩ in control, decreasing to 5.6 ms and 336 MΩ when the presynaptic interneuron was activated.

Presynaptic interneurons were held silent and then depolarized to generate a train of action potentials. At connections with both types of postsynaptic cells, strong facilitation was observed during the presynaptic train of action potentials, with the postsynaptic response reaching a plateau within ~100 ms. Changes in postsynaptic τ_0 and R_{in} caused by activation of the interneuron were assessed using brief current pulses injected when the interneuron was silent and during the plateau of the synaptic response (see Figures 6C and 6D). In Purkinje cells, activating a single presynaptic interneuron decreased apparent τ_0 and R_{in} by 33 ± 5% ($n = 7$; $p < 0.01$) and 37 ± 8% ($p < 0.02$), respectively, relative to control. Similar results were found for postsynaptic interneurons: τ_0 and R_{in} were decreased by 37 ± 6% ($n = 4$; $p < 0.01$) and 30 ± 9% ($p < 0.05$), respectively. The lowest values for postsynaptic τ_0 observed during activity in a single presynaptic interneuron were 9.9 ms for Purkinje cells and 3.2 ms for interneurons.

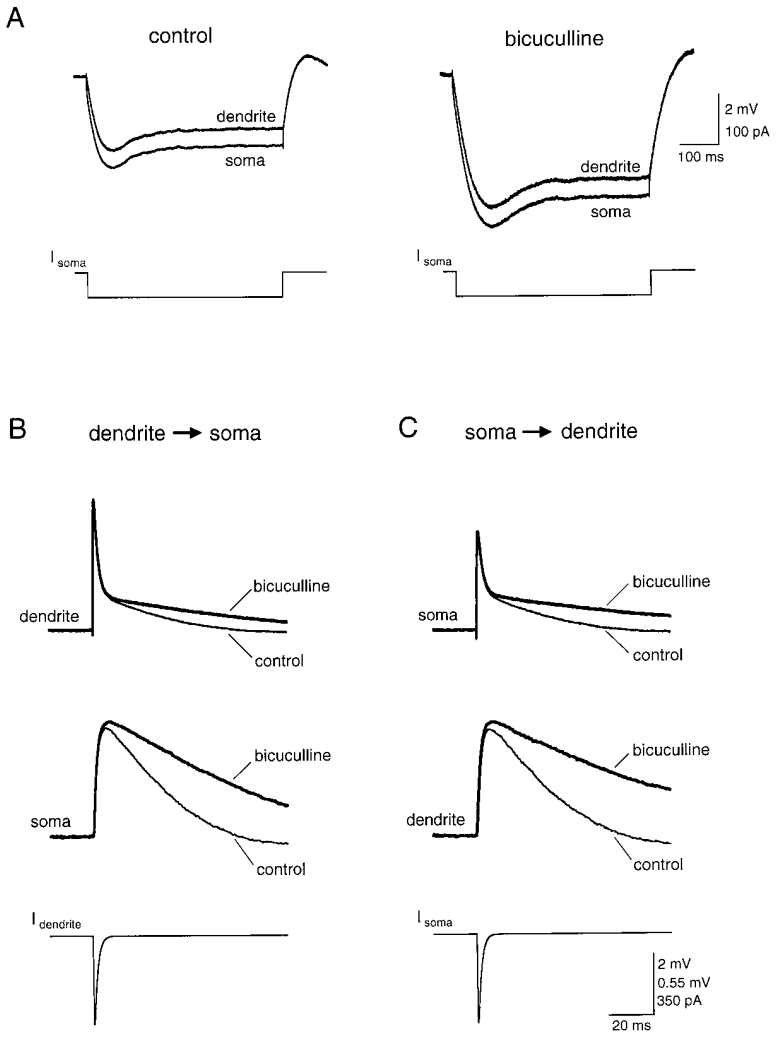

Figure 7. Effect of Tonic Inhibition on Synaptic Integration in Purkinje Cells

(A) Simultaneous somatic and dendritic whole-cell recording from a Purkinje cell. Voltage responses were recorded simultaneously at the soma (bottom trace) and the dendrite (90 μm from the soma; top trace) during a long hyperpolarizing current pulse (100 pA; shown schematically below) injected via the somatic recording pipette. The left section shows the responses under control conditions, and the right section shows the responses after blocking inhibitory synaptic transmission with 30 μM bicuculline. The steady-state attenuation was 75% in control and 84% when inhibition was blocked.

(B and C) Attenuation of simulated synaptic potentials propagating from the dendrite to the soma (B) or from the soma to the dendrite (C); same recording as in (A). In each case, the EPSP at its site of origin is shown in the top traces, and the propagated EPSP is shown in the middle traces; thin lines show the control EPSPs, and thick lines show the EPSPs in the presence of bicuculline. The bottom traces show the time course of the simulated synaptic current. Note the changes in rise time, peak, and decay of the propagated EPSPs when inhibition is blocked.

Tonic Inhibition Affects Synaptic Integration

The experiments described above demonstrate that interneuron activity has important effects on postsynaptic cable properties. How do these changes influence subthreshold synaptic integration? To address this question, simultaneous somatic and dendritic recordings were made from Purkinje cells (Stuart and Häusser, 1994) to examine propagation of potentials within the dendritic tree. We first determined the attenuation of steady-state voltage from the soma into the dendritic tree using long (500–1000 ms) hyperpolarizing somatic current pulses (Figure 7A). Under control conditions, the steady-state voltage at the dendritic recording site (70–120 μm from the soma) was attenuated to 75.9 ± 2.0% of the value at the soma. When spontaneous inhibitory synaptic activity was blocked, the degree of attenuation was reduced to 82.4 ± 3.9% ($n = 9$, $p < 0.01$). This shows that the tonic conductance activated by inhibitory neurons causes an increase in the electrotonic length of Purkinje cell dendrites.

To demonstrate directly how this affects synaptic integration of single excitatory synaptic inputs, excitatory postsynaptic potentials (EPSPs) were simulated by injecting currents with a similar time course to that of the excitatory postsynaptic current (EPSC) via a dendritic pipette (Stuart and Sakmann, 1995). This simulated EPSP was recorded simultaneously at its site of generation (70–120 μm from the soma) as well as at the soma, and EPSP propagation was compared in the presence and absence of inhibition. As shown in Figure 7B, blocking tonic synaptic inhibition produced dramatic changes in the propagation of EPSPs to the soma. The decay of the somatic EPSP was substantially prolonged, with the apparent decay time constant increasing from 34.1 ± 3.9 ms to 67.8 ± 11.9 ms ($p < 0.02$), and the EPSP time integral increasing from 30.3 ± 4.8 mV.ms to 55.9 ± 5.2 mV.ms ($p < 0.01$). These changes were accompanied by an increase in the 20%–80% rise time of the somatic EPSP from 1.17 ± 0.15 ms to 1.35 ± 0.16 ms ($p < 0.01$), and the peak amplitude was also increased from 0.98 ± 0.09 mV to 1.04 ± 0.08 mV ($n = 6$; $p < 0.01$).

Synaptic potentials propagate not only from the dendrites to the soma (centripetal propagation), but also in the opposite direction (centrifugal propagation). To examine the propagation of proximal synaptic potentials into the dendritic tree, synaptic inputs were simulated via the somatic pipette (Figure 7C). Centrifugal propagation of these EPSPs to the dendritic recording site was affected by tonic synaptic activity in a very similar man-

ner to centripetal propagation. When inhibition was blocked, the apparent decay time constant of the EPSP recorded at the dendritic pipette was slowed from 37.4 ± 5.5 ms to 73.7 ± 16.1 ms ($p < 0.03$), and its time integral was increased from 28.8 ± 3.0 mV.ms to 62.8 ± 7.3 mV.ms ($p < 0.01$). The 20%–80% rise time of the dendritic EPSP was also slowed from 1.18 ± 0.16 to 1.45 ± 0.17 ms ($p < 0.01$), and the peak amplitude increased from 0.99 ± 0.10 mV to 1.10 ± 0.12 ms ($p < 0.01$).

Interestingly, at their site of generation, EPSPs were little affected by tonic synaptic inhibition for both somatic and dendritic simulated inputs. Both the 20%–80% rise time and the peak of these "local" EPSPs were unchanged when inhibition was blocked (Figures 7B and 7C, top traces; $p > 0.12$). The decay of the local EPSPs was best fit by a double-exponential function. The dominant fast component (1.69 ± 0.06 ms for dendritic and 1.75 ± 0.07 ms for somatic EPSPs) was comparable to the decay time constant of the simulated synaptic current (Rall, 1967; Jack et al., 1983; Softky, 1994). The slow component (31.2 ± 2.3 ms for dendritic and 36.4 ± 5.3 ms for somatic EPSPs) was very similar to the decay of the propagated EPSP, and therefore reflects the apparent membrane time constant. The fast component was unaffected by blocking inhibition ($p > 0.07$ for dendritic and $p > 0.5$ for somatic EPSPs). As expected, the slow component was significantly prolonged when inhibition was blocked (209 ± 26% increase for dendritic and 200 ± 37% increase for somatic EPSPs; $p < 0.01$ and 0.03, respectively).

Discussion

In this paper, we demonstrate that two GABAergic cell types in the cerebellar cortex, Purkinje cells and molecular layer interneurons, generate action potentials with a regular pattern in the absence of excitatory synaptic input. This spontaneous intrinsic activity has several important consequences. Synaptic input from the spontaneously active inhibitory interneurons transforms the regular firing pattern of Purkinje cells and interneurons into an irregular pattern. The postsynaptic conductance caused by interneuron activity substantially reduces the membrane time constant and input resistance of both cell types, changing the shape and propagation of synaptic potentials. The time window for synaptic integration is thus a dynamic variable that is modulated by the level of activity in the network of inhibitory neurons.

Spontaneous Pacemaker Activity in Purkinje Cells and Interneurons in the Absence of Excitatory Synaptic Input

We have shown using two noninvasive recording techniques that cerebellar Purkinje cells and molecular layer interneurons show spontaneous pacemaker-like action potential firing in the absence of excitatory synaptic input, ruling out the possibility that the spontaneous activity previously observed in Purkinje cells (Llinás and Sugimori, 1980) and interneurons (Midtgaard, 1992a) was due to the shunt induced by microelectrode impalement (Spruston and Johnston, 1992; Staley et al., 1992). Recent reports have also suggested that interneurons may be intrinsically active (Llano and Gerschenfeld, 1993; Vincent and Marty, 1993), consistent with the high rate of inhibitory synaptic currents recorded in Purkinje cells and interneurons (Konnerth et al., 1990; Farrant and Cull-Candy, 1991; Llano and Gerschenfeld, 1993; Vincent and Marty, 1993). Since tetrodotoxin-sensitive spontaneous inhibitory events have been observed at high rates in many different brain regions, such as in the hippocampus (Alger and Nicoll, 1980; Collingridge et al., 1984; Otis et al., 1991; Tóth et al., 1997), cerebral cortex (Salin and Prince, 1996), and in the cerebellar granule cell layer (Brickley et al., 1996), this suggests that endogenous spontaneous activity is a common feature of many GABAergic neurons.

The firing rate of Purkinje cells and interneurons was not significantly reduced by blocking spontaneous excitatory input, consistent with the relatively low rate of spontaneous EPSCs observed in both cell types. Although the slicing procedure probably removes a substantial number of presynaptic granule cells, the major source of excitatory synaptic input to Purkinje cells and interneurons, the low rate of spontaneous excitatory input is also likely to be related to the lack of spontaneous action potential activity observed in granule cells under similar conditions (D'Angelo et al., 1995). Other types of excitatory neurons, such as hippocampal CA1 pyramidal cells (Andersen, 1990; Otmakhov et al., 1993) and neocortical pyramidal cells (Markram et al., 1997), are also quiescent in slice preparations. The difference in spontaneous firing behavior between different neuronal types is most likely due to differences in the expression of voltage-gated channels (Llinás, 1988). Several intrinsic currents are likely to contribute to the pacemaker firing pattern in cerebellar GABAergic neurons, most notably the persistent sodium current, calcium currents, and the hyperpolarization-activated cation current I_h (Llinás, 1988; Llinás et al., 1991; Maccaferri and McBain, 1997; Jaeger et al., 1997). The fact that both Purkinje cells and interneurons showed a wide range of firing rates suggests that the pacemaker mechanism in each cell type is not tightly constrained to produce a particular action potential frequency. However, the low CV for the interspike intervals in the absence of synaptic input indicates that, for a given cell, the intrinsic action potential timing mechanism can be highly precise.

Extracellular recordings from Purkinje cells and molecular layer interneurons in anesthetized animals and in awake animals at rest have shown that these neurons exhibit mean firing rates of 40–50 Hz and 10–30 Hz, respectively (Granit and Phillips, 1956; Eccles et al., 1967; Thach, 1968; Armstrong and Rawson, 1979). These values are comparable to the mean rates that we have measured for the same neurons in the slice preparation, suggesting that some of the observed activity in vivo may be generated by endogenous activation of intrinsic currents, and that few excitatory synaptic inputs are necessary to generate the observed firing rates.

Spontaneous Activity in the Interneuron Population Generates an Irregular Firing Pattern in Purkinje Cells and Interneurons

Spontaneous activity in the interneuron population caused a tonic inhibition of both interneurons and Purkinje cells, in agreement with in vivo recordings showing

that local application of bicuculline increases the firing rate of Purkinje cells (Miyashita and Nagao, 1984; Jaeger and Bower, 1994). Moreover, the highly regular firing pattern of both interneurons and Purkinje cells observed in the absence of synaptic input was transformed into an irregular firing pattern by activity in the population of inhibitory neurons. These findings are consistent with early work on motoneurons suggesting that interspike interval fluctuations are caused primarily by synaptic input (Calvin and Stevens, 1968), as well as with more recent modeling studies (Jaeger et al., 1997) and experiments on immature Purkinje cells in vivo (Bernard and Axelrad, 1993).

The CV of action potential firing ranges from 0.5–1 for Purkinje cells in the awake cat (Armstrong and Rawson, 1979). These values are somewhat larger than those found for Purkinje cells in the slice. The discrepancy is most likely due to the higher levels of synaptic excitation expected in vivo; mixed excitatory and inhibitory input has been shown by modeling studies to substantially raise the CV (Shadlen and Newsome, 1994; Bell et al., 1995; Troyer and Miller, 1997; Jaeger et al., 1997). Values for the CV of interneuron spike trains in vivo are not available; however, they have been reported to fire with a more regular pattern than Purkinje cells, and typically display multiple peaks in their autocorrelograms (Armstrong and Rawson, 1979; Figure 6), as often observed in our recordings from interneurons in the slice preparation.

Single Interneurons Cause Variable Delays in Postsynaptic Action Potentials

We have found that single action potentials in interneurons can, on average, significantly delay the occurrence of a subsequent action potential in both of their major postsynaptic targets, Purkinje cells and interneurons. These results, which confirm and extend preliminary results obtained in turtle Purkinje cells (Midtgaard, 1992b) as well as recent findings in hippocampal pyramidal cells (Miles et al., 1996), demonstrate that single inhibitory neurons can have a significant effect on axonal output of their postsynaptic targets. The longest gaps observed in the spontaneous action potential trains of Purkinje cells and interneurons were considerably longer than the delays produced by individual interneuron action potentials in paired recordings, indicating that inhibition by several presynaptic interneurons summates to produce the longest delays.

Individual interneurons varied widely in their synaptic efficacy at connections with both Purkinje cells and interneurons. The origin of this variability is unknown, but is likely to be related to the number of sites of synaptic contact, their electrotonic location, and their presynaptic release probability (Miles, 1990; Markram et al., 1997). At a given connection, the amplitude of the IPSP also fluctuated substantially from trial to trial, as previously reported at interneuron–Purkinje cell (Vincent and Marty, 1996) and other CNS synapses (Kuno, 1964; Jack et al., 1981; Miles and Wong, 1984; Miles, 1990; Sayer et al., 1990; Mason et al., 1991; Barbour, 1993; Buhl et al., 1994; Markram et al., 1997). We have demonstrated that these trial-to-trial fluctuations at a single connection cause a corresponding variability in the effect of the connection on neuronal output. This result, which was found at both interneuron–Purkinje and interneuron–interneuron synapses, indicates that variability at individual inhibitory connections contributes to the irregularity in spontaneous action potential output observed in both cell types. A relationship between fluctuation of synaptic responses and neuronal output has also been found at excitatory synapses in the hippocampus (Otmakhov et al., 1993). These findings suggest that, by affecting synaptic CV, changing release probability and/or the number of synchronously active synapses will modulate the effect of a given synaptic input on output variability. Comparison with results obtained at other inhibitory synapses demonstrates that the intrinsic membrane properties of the postsynaptic cell can also dramatically affect output variability in response to input: in hippocampal pyramidal neurons, large IPSPs have been shown to interact with intrinsic oscillatory currents to increase the precision of spike timing (Cobb et al., 1995).

Modulation of Synaptic Integration by Single Interneurons and the Interneuron Population

The conductance change generated by activating a single interneuron was sufficient to produce a significant decrease in the apparent membrane time constant and input resistance in postsynaptic Purkinje cells and interneurons. The effect generated by spontaneous activity in the entire presynaptic population of interneurons was substantially greater; in interneurons, the membrane time constant could fall to as low as $\sim$3 ms in the presence of inhibition. Synchronous activation of interneurons, as is expected from the feed-forward circuitry of the cerebellar cortex, should produce even larger effects than those observed here. Blockade of spontaneous excitatory conductances had little additional effect, consistent with the relatively low rate of excitatory input and its modest effect on action potential output under our experimental conditions. These findings provide direct evidence to support theoretical predictions (Barrett, 1975; Holmes and Woody, 1989; Bernander et al., 1991; Rapp et al., 1992) that tonic synaptic input can modulate cable properties. Given that single interneurons can produce significant effects in both interneurons and Purkinje cells, our findings suggest that altering tonic interneuron activity may be a very powerful way to rapidly alter synaptic integration in a population of cells.

The impact of tonic inhibitory input on integration of synaptic potentials was demonstrated directly using simultaneous somatic and dendritic recordings from Purkinje cells. These experiments showed that the tonic inhibitory input increased the electrotonic length of the dendritic tree and consequently increased the attenuation of dendritic inputs as they propagate to the soma into the axon, the final site of synaptic integration (Stuart et al., 1997). Very similar effects were observed for somatic inputs propagating into the dendrites, as expected from theoretical reciprocity relations (Jack et al., 1983; Major et al., 1993). More importantly, the decay of the propagated synaptic responses was substantially accelerated in the presence of inhibition, as expected from

the change in the apparent membrane time constant. This produced a corresponding reduction in the time integral of the propagated synaptic responses, reducing charge transfer from synapse to soma. Interestingly, the EPSP at the site of generation was little affected by tonic inhibition. This is expected since according to passive cable theory, the peak and initial decay of the EPSP at the synapse is not determined by the membrane resistance, but primarily by the local capacitance and the time course of the synaptic current (Rall, 1967; Jack et al., 1983; Softky, 1994). This indicates that local synaptic integration in the dendrites can proceed independently of the level of background synaptic input, at the same time as summation of propagated synaptic potentials can be severely affected.

Functional Implications for Neural Coding

The spontaneous activity of Purkinje cells and interneurons implies that information transmission by these cells is mediated by a modulation of the background firing rate. Since both interneurons and Purkinje cells are GABAergic and inhibitory, this implies that their output is expressed as either an increase or a decrease in the tonic inhibition of their target neurons. Although the idea that the output of the cerebellar cortex is represented by modulation of tonic Purkinje cell firing is central to most theories of cerebellar function (Eccles et al., 1967; Ito et al., 1968; Marr, 1969; Albus, 1971), the finding that much of this tonic activity may be due to spontaneous activity resulting from endogenous currents is relatively unexpected. Instead, previous theories have suggested that the high "resting" firing rate of Purkinje cells is due to integration of activity in excitatory parallel fiber inputs. Determining the relative importance of endogenous activity and excitatory input will require accurate measurements of the rate and patterns of parallel fiber input in vivo.

Whether the irregular firing pattern that we have observed is simply a necessary consequence of a network of spontaneously active, interconnected inhibitory cells, or whether it also serves a functional role in itself, remains unclear at present. The dampening of autorhythmicity by tonic inhibition (see Figures 2 and 3) may help avoid spurious correlations in the output of different neurons firing spontaneously at similar mean frequencies (Perkel et al., 1964). Modeling studies have also shown that networks containing irregularly firing units can respond rapidly, sensitively, and linearly to external inputs (Van Vreeswijk and Sompolinsky, 1996).

Our results provide some clues about the way in which these neurons code synaptic input. The fact that the neurons are close to threshold most of the time implies that their output will be sensitive to relatively small fluctuations in both excitatory and inhibitory synaptic input, as predicted on theoretical grounds (Marr, 1969). This is consistent with our experiments demonstrating that single interneurons can affect output, as well as with previous experiments showing that single granule cells can excite interneurons (Barbour, 1993). While the reduction in the membrane time constant by tonic synaptic inhibition will increase the temporal precision of the coding of synaptic input, tonic synaptic inhibition will also increase jitter in the timing of output spikes. Which effect predominates is likely to depend on the rate and degree of synchronization of the synaptic inputs carrying information. Although Purkinje cells in vivo have been shown to respond reliably to climbing fiber (Eccles et al., 1967; Welsh et al., 1995) and synchronous granule cell input (Eccles et al., 1967; Bower and Woolston, 1983), our findings also suggest that not every action potential conveys information about synaptic input by its precise timing, since action potentials are driven not only by synaptic input but also by endogenous currents (Jaeger et al., 1997). Furthermore, the irregularity of spike trains observed in vivo is unlikely to arise solely through coincidence detection of excitatory synaptic input (Abeles, 1991; Softky and Koch, 1993; Softky, 1994; König et al., 1996), since irregular firing is present already in the slice, where excitatory inputs are largely silent. The fact that these neurons can generate output both endogenously and in response to excitatory input suggests that they may use coincidence detection and rate-coding strategies in parallel. Evaluating this possibility will require a detailed understanding of how reliably the synapses made with the target neurons encode different patterns of activity (Magleby, 1987; Tsodyks and Markram, 1997; Abbott et al., 1997).

Experimental Procedures

Recordings were made from visually identified neurons in 250–350 μm thick slices of cerebellum from 18- to 32-day-old Wistar rats using previously described techniques (Stuart et al., 1993; Stuart and Häusser, 1994). Slices were cut with a vibratome (DTK-1000, Dosaka) in either the sagittal or coronal plane and were perfused continuously with an oxygenated Ringer's solution containing (in mM): 125 NaCl, 25 $NaHCO_3$, 25 glucose, 2.5 KCl, 1.25 NaH_2PO_4, 2 $CaCl_2$, and 1 $MgCl_2$ (pH 7.4 with 5% CO_2). Slices were viewed with an upright microscope (Zeiss Axioskop) using infrared–differential interference contrast optics (Stuart et al., 1993). The identification of Purkinje cells and interneurons is unambiguous and was confirmed in several cases by including biocytin in the recording pipette to reveal the full dendritic morphology of the recorded cell (for methods, see Häusser et al., 1995). All experiments were performed at 35°C ± 1°C.

Recording Spontaneous Action Potential Firing

Cell-attached patch-clamp recordings were made from the soma of Purkinje cells and molecular layer interneurons. The pipette solution for cell-attached recording contained (in mM): 140 K-gluconate, 5 KCl, 10 HEPES, and 1 EGTA (pH 7.3). Extracellular recordings were made using glass pipettes (tip size: 5–10 μM) filled with Ringer's solution. The extracellular recording pipettes were placed under visual control directly adjacent to the soma of the cell of interest. Action currents became indistinguishable from the background noise as the pipette was moved away from the cell soma by several micrometers. Recordings were made with either an Axopatch 200A patch-clamp amplifier (Axon Instruments, Foster City, CA) or with an Axoclamp 2B (Axon Instruments) in voltage-clamp mode. Currents were filtered at 2 kHz and sampled at 20 kHz using a Digidata 1200 A/D converter (Axon Instruments). No differences were found between activity recorded using the two techniques, and therefore results were pooled.

Recording and Detection of Spontaneous Synaptic Currents

Whole-cell voltage-clamp recordings of spontaneous synaptic currents were made from the soma of visually identified interneurons and Purkinje cells using an Axopatch 200A amplifier. Recordings from Purkinje cells were made using pipettes (series resistance 3–9 MΩ during recording) filled with the following solution (in mM): 120

KCl, 10 HEPES, 10 EGTA, 2 Na_2–ATP, and 2 $MgCl_2$ (pH 7.3). Interneurons were recorded from using patch pipettes (series resistance 5–15 MΩ during recording) filled with a solution of the following composition (in mM): 120 K-gluconate, 5 KCl, 10 HEPES, 10 EGTA, 2 Na_2–ATP, 10 Na–phosphocreatine, and 2 $MgCl_2$ (pH 7.3). Series resistance compensation was employed (70%–90%), and recordings were terminated if the series resistance changed >10% over the course of the recording. Synaptic currents were filtered at 1–2 kHz and sampled at 20 kHz. Detection and analysis of synaptic currents was performed semiautomatically using the program NO5 (kindly provided by Steve Traynelis). The detection threshold was set to be the same for each data epoch to be analyzed from a given cell.

Paired Recording from Synaptically Connected Neurons

Simultaneous whole-cell current-clamp recordings were made from the soma of interneurons and Purkinje cells using two identical microelectrode amplifiers (Axoclamp 2B, Axon Instruments). Patch pipettes (10 MΩ for interneurons, 5–7 MΩ for Purkinje cells) were filled with a solution containing (in mM): 125 K-gluconate, 5 KCl, 10 HEPES, 0.1 BAPTA, 2 Na_2–ATP, 2 Mg–ATP, 10 Na–phosphocreatine, 0.3 GTP (Na^+ salt), and 50 U/ml creatine phosphokinase (pH 7.3), which is intended to maintain the physiological intracellular chloride concentration (B. Clark and M. Häusser, 1995, Soc. Neurosci. abstract). Voltage was filtered at 3–5 kHz and sampled at 20 kHz. The connection probability between interneurons and either Purkinje cells or other interneurons was on the order of 10%–15%, and recordings were made at least 30 μm below the surface of the slice. For the experiments investigating the effect of single interneuron spikes on postsynaptic spike timing, the presynaptic interneuron spike was triggered with a fixed latency after a spike in the postsynaptic cell using an event detector (AI 2020A, Axon Instruments). Sweeps with a timed spike in the presynaptic interneuron were alternated with control sweeps in which the presynaptic interneuron was silent. The experiment was terminated when significant changes occurred in the mean interspike interval of the postsynaptic cell. For experiments examining the effect of interneuron activity on τ_0 and R_{in}, the postsynaptic cell was hyperpolarized to −60 to −65 mV, and brief current pulses (0.5 ms) were injected. Grand averages of a large number (≥100) of positive and negative pulses (−1.0 nA and 0.5 nA in Purkinje cells; −0.05 nA and 0.02 nA in interneurons) were constructed (Major et al., 1994). The voltage response was examined on a semilogarithmic plot, and τ_0 was fit by linear regression. The R_{in} was calculated from the impulse response according to the equation:

$$R_{in} = I^{-1} \sum_{n=0}^{n_{max}} C_n (1 - e^{-w/\tau_n})^{-1}$$

(Durand et al., 1983), where I is the amplitude of the injected pulse, w is the duration of the pulse, τ_n is the nth apparent time constant, and C_n is its corresponding amplitude.

Simulating Excitatory Synaptic Input to Purkinje Cells

Simultaneous somatic and dendritic patch-clamp recordings from Purkinje cells were performed as described previously (Stuart and Häusser, 1994). The same internal solution was used as for the paired recordings. EPSPs were simulated by injection of a double-exponential current waveform (Stuart and Sakmann, 1995) with a rising time constant of 0.2 ms and a decaying time constant of 1.5 ms, similar to the time course of spontaneous EPSCs in Purkinje cells (M. Häusser, 1994, Soc. Neurosci., abstract and unpublished data). The peak amplitude of the injected waveform was 500 pA. Somatic access resistances were ≤15 MΩ, and recordings were terminated if the dendritic access resistance exceeded 50 MΩ. Bridge balance and capacitance neutralization were carefully monitored throughout the recording, which was terminated if either of these were not stable over time.

SR 95531 and GYKI 52466 were obtained from RBI, D-AP5 and (S)-methyl-4-carboxyphenylglycine were from Tocris, and all other chemicals were from Sigma. Statistical significance was assessed using the paired Student's *t*-test at the significance level (p) indicated. Pooled data are expressed as mean ± SEM.

Acknowledgments

We are grateful to Philippe Ascher for support and encouragement; Richard Miles and Arnd Roth for helpful discussions; and Philippe Ascher, Zach Mainen, Arnd Roth, Idan Segev, and Greg Stuart for their comments on the manuscript. Supported by the HFSP (M. H.), the European Community (B. A. C.), and the CNRS.

Received June 5, 1997; revised July 18, 1997.

References

Abbott, L.F., Varela, J.A., Sen, K., and Nelson, S.B. (1997). Synaptic depression and cortical gain control. Science *275*, 220–224.

Abeles, M. (1991). Corticonics: Neural Circuits of the Cerebral Cortex. (New York: Cambridge).

Albus, J.S. (1971). A theory of cerebellar function. Math. Biosci. *10*, 25–61.

Alger, B.E., and Nicoll, R.A. (1980). Spontaneous inhibitory postsynaptic potentials in hippocampus: mechanism for tonic inhibition. Brain Res. *200*, 195–200.

Andersen, P. (1990). Synaptic integration in hippocampal CA1 pyramids. In Progress in Brain Research, J. Storm-Mathisen, J. Zimmer, and O. P. Ottersen, eds. (Amsterdam: Elsevier), pp. 215–222.

Armstrong, D.M., and Rawson, J.A. (1979). Activity patterns of cerebellar cortical neurones and climbing fibre afferents in the awake cat. J. Physiol. *289*, 425–448.

Barbour, B. (1993). Synaptic currents evoked in Purkinje cells by stimulating individual granule cells. Neuron *11*, 759–769.

Barrett, J.N. (1975). Motoneuron dendrites: role in synaptic integration. Fed. Proc. *34*, 1398–1407.

Bashir, Z.I., Bortolotto, Z.A., Davies, C.H., Berretta, N., Irving, A.J., Seal, A.J., Henley, J.M., Jane, D.E., Watkins, J.C., and Collingridge, G.L. (1993). Induction of LTP in the hippocampus needs synaptic activation of glutamate metabotropic receptors. Nature *363*, 347–350.

Bell, A.J., Mainen, Z.F., Tsodyks, M., and Sejnowski, T.J. (1995). "Balancing" of conductances may explain irregular cortical spiking. Inst. Neural Comp. Tech. Rep. Ser. INC-9502.

Bernander, Ö., Douglas, R.J., Martin, K.A.C., and Koch, C. (1991). Synaptic background activity influences spatiotemporal integration in single pyramidal cells. Proc. Natl. Acad. Sci. USA *88*, 11569–11573.

Bernard, C., and Axelrad, H. (1993). Effects of recurrent collateral inhibition on Purkinje cell activity in the immature rat cerebellar cortex—an in vivo electrophysiological study. Brain Res. *626*, 234–258.

Bower, J.M., and Woolston, D.C. (1983). Congruence of spatial organization of tactile projections to granule cell and Purkinje cell layers of cerebellar hemispheres of the albino rat: vertical organization of cerebellar cortex. J. Neurophysiol. *49*, 745–766.

Brickley, S.G., Cull-Candy, S.G., and Farrant, M. (1996). Development of a tonic form of synaptic inhibition in rat cerebellar granule cells resulting from persistent activation of $GABA_A$ receptors. J. Physiol. *497*, 753–759.

Buhl, E.H., Halasy, K., and Somogyi, P. (1994). Diverse sources of hippocampal unitary inhibitory postsynaptic potentials and the number of synaptic release sites. Nature *368*, 823–828.

Calvin, W.H., and Stevens, C.F. (1968). Synaptic noise and other sources of randomness in motoneuron interspike intervals. J. Neurophysiol. *31*, 574–587.

Cobb, S.R., Buhl, E.H., Halasy, K., Paulsen, O., and Somogyi, P. (1995). Synchronization of neuronal activity in hippocampus by individual GABAergic interneurons. Nature *378*, 75–78.

Collingridge, G.L., Gage, P.W., and Robertson, B. (1984). Inhibitory post-synaptic currents in rat hippocampal CA1 neurons. J. Physiol. *356*, 551–564.

D'Angelo, E., De Filippi, G., Rossi, P., and Taglietti, V. (1995). Synaptic excitation of individual rat cerebellar granule cells *in situ*: evidence for the role of NMDA receptors. J. Physiol. *484*, 397–413.

Donevan, S.D., and Rogawski, M.A. (1993). GYKI 52466, a 2,3-benzodiazepine, is a highly selective, noncompetitive antagonist of AMPA/kainate receptor responses. Neuron *10*, 51–59.

Durand, D., Carlen, P.L., Gurevich, N., Ho, A., and Kunov, H. (1983). Electrotonic parameters of rat dentate gyrus granule cells measured using short current pulses and HRP staining. J. Neurophysiol. *50*, 1080–1097.

Eccles, J.C., Ito, M., and Szenthagothai, J. (1967). The Cerebellum as a Neuronal Machine (Heidelberg, Germany: Springer).

Farrant, M., and Cull-Candy, S.G. (1991). Excitatory amino acid receptor-channels in Purkinje cells in thin cerebellar slices. Proc. R. Soc. Lond. (Biol.) *244*, 179–184.

Granit, R., and Phillips, C.G. (1956). Excitatory and inhibitory processes acting upon individual Purkinje cells of the cerebellum in cats. J. Physiol. *133*, 520–547.

Hamann, M., Desarmenien, M., Desaulles, E., Bader, M.F., and Feltz, P. (1988). Quantitative evaluation of the properties of a pyridazinyl GABA derivative (SR95531) as a $GABA_A$ competitive antagonist. An electrophysiological approach. Brain Res. *442*, 287–296.

Häusser, M., Stuart, G., Racca, C., and Sakmann, B. (1995). Axonal initiation and active dendritic propagation of action potentials in substantia nigra neurons. Neuron *15*, 637–647.

Holmes, W.R., and Woody, C.D. (1989). Effects of uniform and non-uniform synaptic "activity-distributions" on the cable properties of modeled cortical pyramidal neurons. Brain Res. *505*, 12–22.

Ito, M., Kawai, N., Udo, M., and Sato, N. (1968). Cerebellar evoked inhibition of Deiters neurons. Exp. Brain Res. *2*, 330–349.

Jack, J.J.B., Redman, S.J., and Wong, K. (1981). The components of synaptic potentials evoked in cat spinal motoneurones by impulses in single group Ia afferents. J. Physiol. *321*, 65–96.

Jack, J.J.B., Noble, D., and Tsien, R.W. (1983). Electrical Current Flow in Excitable Cells (Oxford: Oxford University Press).

Jaeger, D., and Bower, J.M. (1994). Prolonged responses in rat cerebellar Purkinje cells following activation of the granule cell layer: an intracellular in vitro and in vivo investigation. Exp. Brain Res. *100*, 200–214.

Jaeger, D., De Schutter, E., and Bower, J.M. (1997). The role of synaptic and voltage-gated currents in the control of Purkinje cell spiking: a modeling study. J. Neurosci. *17*, 91–106.

König, P., Engel, A.K., and Singer, W. (1996). Integrator or coincidence detector? The role of the cortical neuron revisited. Trends Neurosci. *19*, 130–137.

Konnerth, A., Llano, I., and Armstrong, C.M. (1990). Synaptic currents in cerebellar Purkinje cells. Proc. Natl. Acad. Sci. USA *87*, 2662–2665.

Korbo, L., Andersen, B.B., Ladefoged, O., and Møller, A. (1993). Total numbers of various cell types in rat cerebellar cortex using an unbiased stereological method. Brain Res. *609*, 262–268.

Kuno, M. (1964). Quantal components of excitatory postsynaptic potentials in spinal motoneurones. J. Physiol. *175*, 81–99.

Llano, I., and Gerschenfeld, H.M. (1993). Inhibitory synaptic currents in stellate cells of rat cerebellar slices. J. Physiol. *468*, 177–200.

Llinás, R. (1988). The intrinsic electrophysiological properties of mammalian neurons: insights into central nervous system function. Science *242*, 1654–1664.

Llinás, R.R., and Sugimori, M. (1980). Electrophysiological properties of *in vitro* Purkinje cell somata in mammalian cerebellar slices. J. Physiol. *305*, 171–195.

Llinás, R.R., Grace, A.A., and Yarom, Y. (1991). *In vitro* neurons in mammalian cortical layer 4 exhibit intrinsic oscillatory activity in the 10 to 50 Hz frequency range. Proc. Natl. Acad. Sci. USA *88*, 897–901.

Maccaferri, G., and McBain, C.J. (1997). The hyperpolarization-activated current (I_h) and its contribution to pacemaker activity in rat CA1 hippocampal stratum oriens-alveus interneurones. J. Physiol. *497*, 119–130.

Magleby, K.L. (1987). Short-term changes in synaptic efficacy. In Synaptic Function, G.M. Edelman, W.E. Gall, and Cowan, W.M., eds. (New York: Wiley), pp. 21–56.

Major, G., Evans, J.D., and Jack, J.J.B. (1993). Solutions for transients in arbitrarily branching cables: I. Voltage recording with a somatic shunt. Biophys. J. *65*, 423–449.

Major, G., Larkman, A.U., Jonas, P., Sakmann, B., and Jack, J.J.B. (1994). Detailed passive cable models of whole-cell recorded CA3 pyramidal neurons in rat hippocampal slices. J. Neurosci. *14*, 4613–4638.

Markram, H., Lübke, J., Frotscher, M., Roth, A., and Sakmann, B. (1997). Physiology and anatomy of synaptic connections between thick tufted pyramidal neurones in the developing rat neocortex. J. Physiol. *500*, 409–440.

Marr, D. (1969). A theory of cerebellar cortex. J. Physiol. *202*, 437–470.

Mason, A., Nicoll, A., and Stratford, K. (1991). Synaptic transmission between individual pyramidal neurons of the rat visual cortex *in vitro*. J. Neurosci. *11*, 72–84.

McBain, C.J., Eaton, J.V., Brown, T., and Dingledine, R. (1992). CNQX increases spontaneous inhibitory input to CA3 pyramidal neurones in neonatal rat hippocampal slices. Brain Res. *592*, 255–260.

Midtgaard, J. (1992a). Membrane properties and synaptic responses of Golgi cells and stellate cells in the turtle cerebellum *in vitro*. J. Physiol. *457*, 329–354.

Midtgaard, J. (1992b). Stellate cell inhibition of Purkinje cells in the turtle cerebellum *in vitro*. J. Physiol. *457*, 355–367.

Miles, R. (1990). Variation in strength of inhibitory synapses in the CA3 region of guinea-pig hippocampus. J. Physiol. *431*, 659–676.

Miles, R., and Wong, R.K.S. (1984). Unitary inhibitory synaptic potentials in the guinea-pig hippocampus *in vitro*. J. Physiol. *356*, 97–113.

Miles, R., Tóth, K., Gulyás, A.I., Hájos, N., and Freund, T.F. (1996). Differences between somatic and dendritic inhibition in the hippocampus. Neuron *16*, 815–823.

Miyashita, Y., and Nagao, S. (1984). Contribution of cerebellar intracortical inhibition to Purkinje cell response during vestibulo-ocular reflex of alert rabbits. J. Physiol. *351*, 251–262.

Otis, T.S., Staley, K.J., and Mody, I. (1991). Perpetual inhibitory activity in mammalian brain slices generated by spontaneous GABA release. Brain Res. *545*, 142–150.

Otmakhov, N., Shirke, A.N., and Malinow, R. (1993). Measuring the impact of probabilistic transmission on neuronal output. Neuron *10*, 1101–1111.

Palay, S.L., and Chan-Palay, V. (1974). Cerebellar Cortex, Cytology and Organization. (Berlin: Springer).

Perkel, D.H., Gerstein, G., and Moore, G.P. (1964). Pacemaker neurons: effects of regularly spaced synaptic input. Science *145*, 61–63.

Rall, W. (1967). Distinguishing theoretical synaptic potentials computed for different soma-dendritic distributions of synaptic input. J. Neurophysiol. *30*, 1138–1168.

Rapp, M., Yarom, Y., and Segev, I. (1992). The impact of parallel fiber background activity on the cable properties of the cerebellar Purkinje cells. Neural Comput. *4*, 518–533.

Rieke, F., Warland, D., de Ruyter van Steveninck, R., and Bialek, W. (1997). Spikes. (Cambridge, MA: MIT Press).

Salin, P.A., and Prince, D.A. (1996). Spontaneous $GABA_A$ receptor-mediated inhibitory currents in adult rat somatosensory cortex. J. Neurophysiol. *75*, 1573–1588.

Sayer, R.J., Friedlander, M.J., and Redman, S.J. (1990). The time course and amplitude of EPSPs evoked at synapses between pairs of CA3/CA1 neurons in the hippocampal slice. J. Neurosci. *10*, 826–836.

Shadlen, M., and Newsome, W. (1994). Noise, neural codes and cortical organization. Curr. Opin. Neurobiol. *4*, 569–579.

Softky, W. (1994). Sub-millisecond coincidence detection in active dendritic trees. Neuroscience *58*, 13–41.

Softky, W. (1995). Simple codes versus efficient codes. Curr. Opin. Neurobiol. *5*, 239–247.

Softky, W., and Koch, C. (1993). The highly irregular firing of cortical cells is inconsistent with temporal integration of random EPSPs. J. Neurosci. *13*, 334–350.

Spruston, N., and Johnston, D. (1992). Perforated patch-clamp analysis of the passive membrane properties of three classes of hippocampal neurons. J. Neurophysiol. *67*, 508–529.

Spruston, N., Jaffe, D.B., and Johnston, D. (1994). Dendritic attenuation of synaptic potentials and currents: the role of passive membrane properties. Trends Neurosci. *17*, 161–166.

Staley, K., Otis, T.S., and Mody, I. (1992). Membrane properties of dentate gyrus granule cells: comparison of sharp microelectrode and whole cell recordings. J. Neurophysiol. *67*, 1346–1358.

Stuart, G., and Häusser, M. (1994). Initiation and spread of sodium action potentials in cerebellar Purkinje cells. Neuron *13*, 703–712.

Stuart, G., and Sakmann, B. (1995). Amplification of EPSPs by axosomatic sodium channels in neocortical pyramidal neurons. Neuron *15*, 1065–1076.

Stuart, G.J., Dodt, H.-U., and Sakmann, B. (1993). Patch-clamp recordings from the soma and dendrites of neurons in brain slices using infrared video microscopy. Pflügers Arch. *423*, 511–518.

Stuart, G., Spruston, N., Sakmann, B., and Häusser, M. (1997). Action potential initiation and backpropagation in neurons of the mammalian CNS. Trends Neurosci. *20*, 125–131.

Thach, W.T. (1968). Discharge of Purkinje cells and cerebellar nuclear neurons during rapidly alternating arm movements in the monkey. J. Neurophysiol. *31*, 785–797.

Tóth, K., Freund, T.F., and Miles, R. (1997). Disinhibition of rat hippocampal pyramidal cells by GABAergic afferents from the septum. J. Physiol. *500*, 463–474.

Troyer, T.W., and Miller, K.D. (1997). Physiological gain leads to high isi variability in a simple model of a cortical regular spiking cell. Neural Comput. *9*, 733–745.

Tsodyks, M.V., and Markram, H. (1997). The neural code between neocortical pyramidal neurons depends on neurotransmitter release probability. Proc. Natl. Acad. Sci. USA *94*, 719–723.

Ueno, S., Bracamontes, J., Zorumski, C., Weiss, D.S., and Steinbach, J.H. (1997). Bicuculline and gabazine are allosteric inhibitors of channel opening of the $GABA_A$ receptor. J. Neurosci. *15*, 625–634.

Van Vreeswijk, C., and Sompolinsky, H. (1996). Chaos in neuronal networks with balanced excitatory and inhibitory activity. Science *274*, 1724–1726.

Vincent, P., and Marty, A. (1993). Neighboring cerebellar Purkinje cells communicate via retrograde inhibition of common presynaptic interneurons. Neuron *11*, 885–893.

Vincent, P., and Marty, A. (1996). Fluctuations of inhibitory postsynaptic currents in Purkinje cells from rat cerebellar slices. J. Physiol. *494*, 183–199.

Welsh, J.P., Lang, E.J., Sugihara, I., and Llinás, R. (1995). Dynamic organization of motor control within the olivocerebellar system. Nature *374*, 453–457.

Zorumski, C.F., Yamada, K.A., Price, M.T., and Olney, J.W. (1993). A benzodiazepine recognition site associated with the non-NMDA glutamate receptor. Neuron *10*, 61–67.